fractal and fractional

MDPI

Article

Theoretical Analysis and Simulation of a Fractional-Order Compartmental Model with Time Delay for the Propagation of Leprosy

Zafar Iqbal [1], Nauman Ahmed [1] and Jorge E. Macías-Díaz [2,3,*]

[1] Department of Mathematics and Statistics, The University of Lahore, Lahore 54590, Pakistan
[2] Department of Mathematics and Didactics of Mathematics, School of Digital Technologies, Tallinn University, Narva Rd. 25, 10120 Tallinn, Estonia
[3] Departamento de Matemáticas y Física, Universidad Autónoma de Aguascalientes, Avenida Universidad 940, Ciudad Universitaria, Aguascalientes 20131, Ags., Mexico
* Correspondence: jorge.macias_diaz@tlu.ee; Tel.: +52-449-910-8400

Abstract: This article investigates the propagation of a deadly human disease, namely leprosy. At the outset, the mathematical model is transformed into a fractional-order model by introducing the Caputo differential operator of arbitrary order. A result is established, which ensures the positivity of the fractional-order epidemic model. The stability of the continuous model at different points of equilibria is investigated. The basic reproduction number, R_0, is obtained for the leprosy model. It is observed that the leprosy system is locally asymptotically stable at both steady states when $R_0 < 1$. On the other hand, the fractional-order system is globally asymptotically stable when $R_0 > 1$. To find the approximate solutions for the continuous epidemic model, a non-standard numerical scheme is constructed. The main features of the non-standard scheme (such as positivity and boundedness of the numerical method) are also confirmed by applying some benchmark results. Simulations and a feasible test example are presented to discern the properties of the numerical method. Our computational results confirm both the analytical and the numerical properties of the finite-difference scheme.

Keywords: fractional epidemic model; leprosy infection with memory effects; non-standard finite-difference scheme; local and stability analyses; numerical simulations

MSC: 30G35; 35F15; 31B10; 74B05; 35Q60

check for updates

Citation: Iqbal, Z.; Ahmed, N.; Macías-Díaz, J.E. Theoretical Analysis and Simulation of a Fractional-Order Compartmental Model with Time Delay for the Propagation of Leprosy. *Fractal Fract.* **2023**, *7*, 79. https://doi.org/10.3390/fractalfract7010079

Received: 23 November 2022
Revised: 20 December 2022
Accepted: 5 January 2023
Published: 10 January 2023

Copyright: © 2023 by the authors. Licensee MDPI, Basel, Switzerland. This article is an open access article distributed under the terms and conditions of the Creative Commons Attribution (CC BY) license (https://creativecommons.org/licenses/by/4.0/).

1. Introduction

Historically, the word *leprosy* is derived from the Greek word *lepra*; it is a human disease that is also known as Hansen's disease. This infection is caused by *mycobacterium leprae* and *mycobacterium lepromatosis*, and it is a long-term infection which leads to the damage of the respiratory tract, nerves, eyes, and skin. According to the World Health Organization (WHO), most of the people affected by leprosy nowadays are found in Africa and Asia. Moreover, about 100 people affected by this disease are found in the U.S. every year. It is worth recalling here that there are two major types of leprosy, namely lepromatous and tuberculoid. Persons affected with the first kind of leprosy usually present a large amount of bacteria in the organism, while the second type is characterized by a smaller amount. Lepromatous is the more dangerous type of leprosy. Some of the complications from this disease are the loss of sensation and anomalies present in the hands, feet, and face. The kidney, the nose, and the male reproductive organ are also affected by this disease.

In general, leprosy firstly affects the skin, eyes, nose, nerves, and peripheral nerves. The symptoms for this disease appear approximately 3–5 years after the first contact with the mycobacterium. Thirty percent of people affected by leprosy experience nerve damage,

which may lead to paralysis, numbness, ulceration, and joint deformation. If detected at the early stages, medication may reduce the risk of leprosy for those who come in contact with the leprosy patient. From a medical point of view, the prevention of leprosy hinges on a single dose of rifampicin (SDR). This approach reduces the risk of infection up to 57 percent in 2 years, and 30 percent after 6 years. The WHO recommended the Bacillus Calmette-Gurin (BCG) vaccine for protection from leprosy, which is 26–41 percent effective. Secondary effects include blindness, kidney failure, muscle weakness, hair loss, and the permanent damage of peripheral nerves. From the bacteriological point of view, leprosy is caused by *mycobacterium leprae* or *mycobacterium leprometosis*, which are both clinically undistinguished.

From a mathematical point of view, Mazza, Pastore, and De-Souza [1] investigated some mathematical and computational models in 2019 for the dynamics of the propagation of leprosy. In the article, the authors presented and analyzed some compartmental epidemic models that considered transmission in new patients, the spatial dispersion of leprosy in population, and the planning for disease control strategies. In 2013, Peters et al. studied the meaning of leprosy and everyday experiences through a particular study case [2]. In 2016, Matos et al. elucidated future preventive interventions for new cases of leprosy in Pará state, Brazil [3]. The SIMCOLEP, an existing individual-based model, was used to study the transmission and control of *mycobacterium leprae* in a human population. The control of leprosy with the use of chemoprophylaxis and the discontinuation of contact tracing were investigated. Chivaka and coworkers also investigated the transmission dynamics of leprosy [4]. More concretely, they studied the non-complying behavior of patients and the inadequate treatment of this disease. They proposed a deterministic mathematical model that would encapsulate inadequate treatment and non-compliance with the precautionary measures.

Mushayabasa et al. [5] worked on the modeling effect of chemotherapy on the transmission of leprosy dynamics in 2012. A mathematical model for leprosy treatment and its transmission among asymptomatic and symptomatic individuals was developed in that work. The effect of leprosy relapse and compliance with the therapy of individual and administrative was considered therein. On the other hand, Abubakar and coworkers proposed a Markov decision model as a theoretical framework to elucidate the cost of treatment of leprosy [6]. In 2013, Enagi et al. presented a deterministic model, in which the disease-free and endemic equilibria were calculated, and the respective stability analyses were theoretically carried out [7]. Lietman et al. [8] proposed a mathematical model for the transmission dynamics of tuberculosis and leprosy.

From the perspective of the immunology of the disease, Walker and coworkers showed that leprosy infection can be cured by MDT, but that it may lead to immunological reactions, disability, and deformations as a result of neuropathy caused by rapid treatment [9]. In 2015, Egli et al. presented a mathematical model for the prediction of leprosy incidence and the effect of intervention strategies [10]. Smith et al. studied leprosy dynamics using a deeper understanding of the biology of the infection [11]. These authors introduced a compartment-based continuous model that employed approximate Bayesian computations to determine the rate of detection and the transmission coefficients. In 2013, Hohmann et al. investigated a hypothesis on the clinical outcomes of the co-infection leprosy-tuberculosis by means of mathematical modeling [12]. Later on, Meima and coauthors investigated a simulation model for leprosy and discussed its transmission control in a population along with its potential applications and limitations [13]. In 2015, Donoghue et al. studied the historical spread of leprosy in Central Europe and medieval Eastern areas by using a migration-driven mathematical model [14]. Finally, in 2019, Haroun and coworkers studied a deep phenotype in India and investigated the clinical characteristics of neuropathic pain in leprosy and associated somatosensory profiles [15].

The classical derivatives are local in nature, so they can measure the changes at a specific moment in time, while the fractional-order derivatives are non-local in nature and involve the memory effect. Therefore, they can clearly depict the system behavior [16].

Moreover, some researchers observed that the fractional-order epidemic models fit better with the real data and enhance the stability of the solutions [17].

Huang et al. studied the issues of bifurcations from fractional-order neural network systems with different types of delays [18,19]. Similarly, Li et al. worked on the stability property and Hopf bifurcation of fractional-order genetic regulatory networks by considering the distributed and discrete delays in the system [20].

In the present work, we investigate the transmission dynamics of leprosy in a human population using a compartmental epidemic model. The model proposed in this work considers the presence of susceptible and asymptomatic individuals. Moreover, we categorize the sub-populations of infected individuals into multibacillary leprosy and paucibacillary leprosy. These four disjoint compartments constitute the total population under study, and memory effects are considered for the sake of generality. Various theoretical results are established in this work, such as the existence of disease-free and endemic equilibrium solutions along with their stability properties. The basic reproduction number is derived to this end using the next-generation matrix approach. To confirm our analytical results, we propose a non-standard finite-difference method to approximate the solutions of the model. Some relevant properties on the discretization are established theoretically, such as the capability of the methodology to preserve the positivity and the boundedness. By means of a computational implementation, we show that the methodology is capable of preserving the positivity and boundedness, and that it is able to identify the equilibrium solutions and their stability properties. In this way, the theoretical results derived in this work are computationally confirmed.

2. Mathematical Model

In this section, we will introduce a mathematical model that describes the dynamics of propagation of the leptospirosis disease. To that end, we considered a human population divided into four disjoint compartments. Let $x(t)$ represent the sub-population size of susceptible individuals at time $t \geq 0$, while $y(t)$ denotes the sub-population size of asymptomatic persons who have been infected by multibacillary or paucibacillary leprosy. Let us also assume that $z(t)$ represents the the number of individuals infected by multibacillary leprosy and $w(t)$ the number of people infected by paucibacillary leprosy at time t. Moreover, suppose that $n(t)$ represents the population size at time t.

In this work, assume that f represents the fraction of people who developed multibacillary leprosy, so that $1-f$ represents the fraction of people who developed paucibacillary leprosy. Let τ denote a temporal delay, ρ is the annual net growth rate, β_ρ represents the effective contact rate for paucibacillary leprosy transmission, β_m denotes the active contacting rate for multibacillary leprosy dynamics, θ is the rate of transfer from the no-symptoms stage to the stage of leprosy, μ_m is the population death rate of infected individuals with multibacillary leprosy, and μ represents the natural death rate. We suppose that all of these parameters are positive and constant throughout time. Under these conventions, we depart from the following integer-order mathematical model for the spread of leprosy:

$$\frac{dx(t)}{dt} = \rho - \left(\beta_m x(t)\frac{z(t-\tau)}{N} + \beta_\rho x(t)\frac{w(t-\tau)}{N}\right)e^{-\mu\tau} - \mu x(t), \qquad \forall t \geq 0, \tag{1}$$

$$\frac{dy(t)}{dt} = \left(\beta_m x(t)\frac{z(t-\tau)}{N} + \beta_\rho x(t)\frac{w(t-\tau)}{N}\right)e^{-\mu\tau} - \theta y(t) - \mu y(t), \qquad \forall t \geq 0, \tag{2}$$

$$\frac{dz(t)}{dt} = f\theta y(t) - \mu_m z(t), \qquad \forall t \geq 0, \tag{3}$$

$$\frac{dw(t)}{dt} = (1-f)\theta y(t) - \mu w(t), \qquad \forall t \geq 0. \tag{4}$$

Evidently, this is a delayed system of ordinary differential equations that is nonlinearly coupled.

We wish to extend this mathematical model to the fractional-order scenarios. To that end, it is important to point out beforehand that there are many fractional operators

reported in the literature. Among those operators, the Caputo fractional derivative has traditionally been used in order to account for memory effects. More precisely, if ξ is any positive real number and $\Phi : [0, \infty) \to \mathbb{R}$ is a sufficiently smooth function, then the Caputo derivative of Φ of order ξ at time t is defined as follows:

$$ {}_0^C D_t^\xi \Phi(t) = \frac{1}{\Gamma(k-\xi)} \int_0^t (t-\tau)^{k-\xi-1} \frac{d^k}{dt^k} \Phi(\tau) d\tau, \tag{5} $$

where $k = [\xi] + 1$ obviously satisfies the relation $k - 1 < \xi \leq k$, and Γ is the usual Gamma function that extends factorials and is represented by $\Gamma(z) = \int_0^\infty e^{-t} t^{z-1} \mathrm{dt}$. With these conventions, the fractional-order generalization of the integer-order leprosy model is given by the following delayed system of ordinary differential equations:

$$ {}_0^C D_t^\xi x(t) = \rho^\xi - \left(\beta_m^\xi x(t) \frac{z(t-\tau)}{N} + \beta_\rho^\xi x(t) \frac{w(t-\tau)}{N} \right) e^{-\mu\tau} - \mu^\xi x(t), \tag{6} $$

$$ {}_0^C D_t^\xi y(t) = \left(\beta_m^\xi x(t) \frac{z(t-\tau)}{N} + \beta_\rho^\xi x(t) \frac{w(t-\tau)}{N} \right) e^{-\mu\tau} - \theta^\xi y - \mu^\xi y(t), \tag{7} $$

$$ {}_0^C D_t^\xi z(t) = f^\xi \theta^\xi y(t) - \mu_m^\xi z(t), \tag{8} $$

$$ {}_0^C D_t^\xi w(t) = (1 - f^\xi) \theta^\xi y(t) - \mu^\xi w(t), \tag{9} $$

for all $t \geq 0$. For the sake of completeness, we will impose non-negative initial data of the form $x(0) = x_0 \geq 0$, $y(0) = y_0 \geq 0$, $z(0) = z_0 \geq 0$ and $w(0) = w_0 \geq 0$. Moreover, notice that we are emphasizing the dependence of the parameters on the differentiation order ξ in this last system of differential equations.

Theorem 1. *The solution of systems* (6)–(9) *are positive-invariant.*

Proof. Notice that the following identities are satisfied for systems (6)–(9):

$$ {}_0^C D_t^\xi x(t)|_{x=0} = \rho^\xi, \qquad \forall t \geq 0, \tag{10} $$

$$ {}_0^C D_t^\xi y(t)|_{y=0} = \left(\beta_m^\xi x(t) \frac{z(t-\tau)}{N} + \beta_\rho^\xi x(t) \frac{w(t-\tau)}{N} \right) e^{-\mu\tau}, \qquad \forall t \geq 0, \tag{11} $$

$$ {}_0^C D_t^\xi z(t)|_{z=0} = f^\xi \theta^\xi y(t), \qquad \forall t \geq 0, \tag{12} $$

$$ {}_0^C D_t^\xi w(t)|_{w=0} = (1 - f^\xi) \theta^\xi y(t), \qquad \forall t \geq 0. \tag{13} $$

As a consequence, observe that the vector field points into $\mathbb{R}^4_+$ on each hyperplane bounding the non-negative hyper-octant. The positivity of the solutions now readily follows. □

Theorem 2. *The solutions of systems* (6)–(9) *are bounded.*

Proof. Once we have proved that the system has positive solutions, the result is straightforward. Indeed, sum the four equations of the fractional-order epidemic model and cancel out the term. An inequality bounding ${}_0^C D_t^\xi n(t)$ from above will be obtained, from where the boundedness will readily follow. □

Next, we examine the equilibrium solutions for systems (6)–(9).

Definition 1. *Consider a Caputo fractional system of ordinary differential equations of the form* ${}_0^C D_t^\xi u(t) = \mathcal{F}(t, u(t))$. *We say that a point* u^* *is an* equilibrium solution *for this system if* $\mathcal{F}(t, u^*(t)) = 0$.

Following this definition, systems (6)–(9) have two equilibrium solutions, namely the disease-free equilibrium solution $(x^0, y^0, z^0, w^0) = (\frac{\rho}{\mu}, 0, 0, 0)$ and the endemic equilibrium (x^*, y^*, z^*, w^*), where the components are given by the following equations:

$$x^* = \frac{u(\theta+u)}{\beta_m f\theta + \beta_p\theta(1-f)}, \tag{14}$$

$$y^* = \frac{[\beta_m f\theta + \beta_p\theta(1-f)]\rho e^{-\mu\tau} - \mu^2(\theta+\mu)}{(\theta+\mu)[\beta_m f\theta + \beta_p\theta(1-f)]e^{-\mu\tau}]}, \tag{15}$$

$$w^* = \frac{\theta(1-f)}{u}\frac{[\beta_m f\theta + \beta_p\theta(1-f)]\rho e^{-\mu\tau} - \mu^2(\theta+\mu)}{(\theta+\mu)[\beta_m f\theta + \beta_p\theta(1-f)]e^{-\mu\tau}]}, \tag{16}$$

$$z^* = \frac{f\theta}{u}\frac{[\beta_m f\theta + \beta_p\theta(1-f)]\rho e^{-\mu\tau} - \mu^2(\theta+\mu)}{(\theta+\mu)[\beta_m f\theta + \beta_p\theta(1-f)]e^{-\mu\tau}}. \tag{17}$$

In order to calculate the basic reproductive number, we use the well-known next-generation matrix approach. To that end, we define the auxiliary matrices as follows:

$$A = \begin{pmatrix} 0 & \beta_m\frac{\rho}{\mu}e^{-\mu\tau} & \beta_p\frac{\rho}{\mu}e^{-\mu\tau} \\ 0 & 0 & 0 \\ 0 & 0 & 0 \end{pmatrix}$$

and

$$B = \begin{pmatrix} \theta+\mu & 0 & 0 \\ -f\theta & \mu & 0 \\ -\theta(1-f) & 0 & \mu \end{pmatrix}$$

Under these conventions, the basic reproductive number, R_0, is the largest eigenvalue of the matrix AB^{-1}. It is easy to check algebraically that the value of R_0 for systems (6)–(9) is given by the equation below:

$$R_0 = \left(\frac{\beta_m f\theta + \beta_p\theta(1-f)}{\mu^2(\theta+\mu)}\right)\rho e^{-\mu\tau}. \tag{18}$$

3. Analytical Results

The present section provides the local and global stability analyses for the equilibrium points derived in the previous section. In this sense, the following definition is of utmost importance.

Definition 2. *An equilibrium point u^* of the system ${}_0^C D_0^\xi u(t) = \mathcal{F}(t, u(t)), u(t_0) > 0$ is* locally asymptotically stable *if each of the eigenvalues λ of the Jacobian matrix of the function $\mathcal{F}$ evaluated at the equilibrium point satisfies the inequality $|\arg\lambda| > \frac{\xi\pi}{2}$.*

Theorem 3. *The disease-free equilibrium solution of the fractional-order leprosy model is locally asymptotically stable provided that $R_0 < 1$, and unstable when $R_0 > 1$.*

Proof. Beforehand, notice that the disease-free equilibrium point $D_1 = (x^0, y^0, z^0, w^0)$ of systems (6)–(9) is locally asymptotically stable whenever the eigenvalues λ_i are negative, with $|\arg\lambda_i| > \frac{\xi\pi}{2}$ for each $i = 1, 2, 3, 4$. Notice that the Jacobian matrix J at point D_1 is given by the following equation:

$$J(D_1) = \begin{pmatrix} -\mu & 0 & -\beta_m\frac{\rho}{\mu}e^{-\mu\tau} & -\beta_p\frac{\rho}{\mu}e^{-\mu\tau} \\ 0 & -\theta-\mu & \beta_m\frac{\rho}{\mu}e^{-\mu\tau} & \beta_p\frac{\rho}{\mu}e^{-\mu\tau} \\ 0 & f\theta & -\mu_m & 0 \\ 0 & \theta(1-f) & 0 & -\mu \end{pmatrix}. \tag{19}$$

It is easy to see that one of the eigenvalues is $\lambda_1 = -\mu < 0$. Let us define the following auxiliary constants:

$$a_1 = \theta + \mu, \tag{20}$$

$$a_2 = \beta_m \frac{\rho}{\mu} e^{-\mu\tau}, \tag{21}$$

$$a_3 = \beta_p \frac{\rho}{\mu} e^{-\mu\tau}, \tag{22}$$

$$a_4 = \theta(1-f). \tag{23}$$

Then, the remaining eigenvalues satisfy the cubic polynomial

$$\lambda^3 + A_1\lambda^2 + A_2\lambda + A_3 = 0, \tag{24}$$

where

$$A_1 = a_1 + 2\mu, \tag{25}$$

$$A_2 = 2a_1\mu + \mu^2 - a_2 f\theta - a_3 a_4, \tag{26}$$

$$A_3 = a_1\mu^2 - a_2 f\theta\mu - a_3\mu a_4. \tag{27}$$

We will now use the Routh–Hurwitz criterion for cubic polynomials after observing that $A_2 > 0$, $A_0 > 0$, and $A_2A_0 > A_1$ whenever $R_0 < 1$. As a consequence, all the eigenvalues are negative. Hence, the equilibrium point D_1 of systems (6)–(9) is locally asymptotically stable. □

Theorem 4. *The endemic equilibrium point of the fractional-order leprosy model is locally asymptotically stable when $R_0 > 1$, and unstable when $R_0 < 1$.*

Proof. Notice that the endemic point $E_1 = (x^*, y^*, z^*, w^*)$ is locally asymptotically stable when every eigenvalue λ_i of the Jacobian matrix at E_1 is negative, and $|\arg\lambda_i| > \frac{\zeta\pi}{2}$ for each $i = 1, 2, 3, 4$. Firstly, take note that the Jacobian matrix at E_1 is given as follows:

$$J(E_1) = \begin{pmatrix} -(\beta_m z^* + \beta_p w^*)e^{-\mu\tau} - \mu & 0 & \beta_m x^* e^{-\mu\tau} & -\beta_p x^* e^{-\mu\tau} \\ (\beta_m z^* + \beta_p w^*)e^{-\mu\tau} & -\theta - \mu & \beta_m x^* e^{-\mu\tau} & \beta_p x^* e^{-\mu\tau} \\ 0 & f\theta & -\mu_m & 0 \\ 0 & \theta(1-f) & 0 & -\mu \end{pmatrix}.$$

As a consequence, the characteristic polynomial of this matrix is given by the following quartic equation:

$$\lambda^4 + B_1\lambda^3 + B_2\lambda^2 + B_3\lambda + B_4 = 0, \tag{28}$$

where the coefficients are defined as follows:

$$B_1 = b_1 + b_4 + 2b_6 + \mu, \tag{29}$$

$$B_2 = b_3b_7 - b_1b_6 - b_6\mu - b_6^2 - b_4b_6 + b_2b_5 - b_1b_6 - b_1b_4 - b_6\mu - b_4\mu - b_4b_6, \tag{30}$$

$$B_3 = b_3b_6b_7 + b_3\mu b_7 + b_2b_6b_5 - b_1b_6^2 - b_1b_4b_6 - \mu b_6^2 - b_4b_6^2 - b_4b_6\mu + b_2b_5\mu - b_1b_4b_6 - b_4b_6\mu, \tag{31}$$

$$B_4 = b_3b_7b_6\mu + b_2b_5b_6\mu + b_1b_4b_6^2\mu, \tag{32}$$

and

$$b_1 = (\beta_m z^* + \beta_p w^*)e^{-\mu\tau}, \tag{33}$$
$$b_2 = \beta_m x^* e^{-\mu\tau}, \tag{34}$$
$$b_3 = \beta_p x^* e^{-\mu\tau}, \tag{35}$$
$$b_4 = \theta + \mu, \tag{36}$$
$$b_5 = f\theta, \tag{37}$$
$$b_6 = \mu, \tag{38}$$
$$b_7 = \theta(1-f). \tag{39}$$

The conclusion now readily follows by using the Routh–Hurwitz criterion for quartic polynomials. □

Next, we examine the global asymptotic stability of the equilibrium solutions.

Theorem 5. *For the fractional-order leprosy systems (6)–(9), the disease-free equilibrium exhibits global asymptotic stability when $R_0 < 1$.*

Proof. Following the approach reported in [15,21] and using the fact that $S(t) \leq \frac{\rho}{\mu}$ for each $t \geq 0$, the rate of change of the variables (x, z, w) in systems (6)–(9) satisfies the following:

$$\begin{pmatrix} y \\ z \\ w \end{pmatrix} = (A-B)\begin{pmatrix} y \\ z \\ w \end{pmatrix} - \left(1 - \frac{\mu}{\rho}S\right)A\begin{pmatrix} y \\ z \\ w \end{pmatrix} \leq (A-B)\begin{pmatrix} y \\ z \\ w \end{pmatrix}. \tag{40}$$

Here, A and B are the same matrices used in the calculation of the basic reproductive number. As a consequence of Theorem 3, it is easy to see now that systems (6)–(9) are stable whenever $R_0 < 1$. Thus, $(y, z, w) \to (0, 0, 0)$ as $t \to \infty$. By the comparison theorem used in [15,22], it follows that $(y, z, w) \to (0, 0, 0)$ and $S \to \frac{\rho}{\mu}$ as $t \to \infty$. Then, $(x, y, z, w) \to D_1$ as $t \to \infty$, which means that D_1 is globally asymptotically stable if $R_0 < 1$. □

Theorem 6. *The endemic equilibrium is globally asymptotically stable if $R_0 > 1$.*

Proof. We follow the approach described in [23]. To that end, recall that the endemic equilibrium is the point $E_1 = (x^*, y^*, z^*, w^*)$, and consider the following Lyapunov function:

$$\begin{aligned} U(t) = &\left(x - x^* - x^* \ln \frac{x^*}{x}\right) + \left(y - y^* - y^* \ln \frac{y^*}{y}\right) + \left(z - z^* - z^* \ln \frac{z^*}{z}\right) \\ &+ \left(w - w^* - w^* \ln \frac{w^*}{w}\right). \end{aligned} \tag{41}$$

Bounding from above and using the linearity of the Caputo fractional operator, it is easy to check that the following inequalities are satisfied:

$$\begin{aligned}
{}_0^C D_t^\xi U(t) &\leq \left(1-\frac{x^*}{x}\right){}_0^C D_0^\xi x(t) + \left(1-\frac{y^*}{y}\right){}_0^C D_0^\xi y(t) + \left(1-\frac{z^*}{z}\right){}_0^C D_t^\xi z(t) \\
&\quad + \left(1-\frac{w^*}{w}\right){}_0^C D_0^\xi w(t) \\
&\leq (x-x^*)\left[\frac{\rho}{x} - \frac{\beta_m z e^{-\mu\tau}}{N} - \frac{\beta_p w e^{-\mu\tau}}{N} - \frac{\rho}{x^*} + \frac{\beta_m z^* e^{-\mu\tau}}{N} + \frac{\beta_p w^* e^{-\mu\tau}}{N}\right] \\
&\quad + (y-y^*)\left[\frac{\beta_m x z e^{-\mu\tau}}{yN} + \frac{\beta_p x w e^{-\mu\tau}}{yN} - \frac{\beta_m x z e^{-\mu\tau}}{y^* N} - \frac{\beta_p x w e^{-\mu\tau}}{y^* N}\right] \\
&\quad + (z-z^*)\left[\frac{f\theta y}{z} - \frac{f\theta y}{z^*}\right] + (w-w^*)\left[\frac{\theta(1-f)y}{w} - \frac{\theta(1-f)y}{w^*}\right] \\
&\leq \frac{\rho(x-x^*)^2}{xx^*} - \frac{\beta_m e^{-\mu\tau}}{N}(x-x^*)(z-z^*) - \frac{\beta_p e^{-\mu\tau}}{N}(x-x^*)(w-w^*) \\
&\quad - \frac{(y-y^*)^2}{yy^*N}\beta_m x z e^{-\mu\tau} - \frac{(y-y^*)^2}{yy^*N}\beta_p x w e^{-\mu\tau} - \frac{(z-z^*)^2}{zz^*} f\theta y \\
&\quad - \frac{(w-w^*)^2\theta(1-f)y}{ww^*}.
\end{aligned} \tag{42}$$

It follows that ${}_0^C D_0^\xi U(t) \leq 0$ if $R_0 > 1$, and ${}_0^C D_0^\xi D_t^{r^*,\theta} = 0$ only in the case when $x = x^*$, $y = y^*$, $z = z^*$, and $w = w^*$. By Lasalle's invariance principle, we conclude that the endemic equilibrium solution is globally asymptotically stable, as desired. □

4. Numerical Results

The purpose of this section is to propose and analyze a hybridized numerical scheme to approximate the solutions for our fractional-order leprosy model (6)–(9). To that end, we employ the Grünwald–Letnikov (GL) approximation combined with a non-standard finite-difference scheme obtained by following Micken's rules. For further details, we refer the reader to [24,25]. Therefore, let us consider the fraction leprosy system (6)–(9).

Let $\kappa > 0$ be a temporal step size, and let $t_j = j\kappa$ for each $j \in \mathbb{N} \cup \{0\}$. Moreover, let us agree that $x_j = x(t_j)$ for each $j \in \mathbb{N} \cup \{0\}$. To start with, let us remember that the GL scheme is used to approximate fractional derivatives of the Caputo type. More precisely, for the function x in our mathematical model, the fractional derivative of order ξ is approximated as follows:

$${}_0^C D_t^\xi x(t) = \frac{1}{\psi(\kappa)^\xi}\left(x_{j+1} - \sum_{i=1}^{j+1} e_i x_{j+1-i} - \mathfrak{r}_{j+1} x_0\right), \qquad \forall j \geq 0. \tag{43}$$

Here, $\psi : \mathbb{R} \to \mathbb{R}$ is a suitable function. By applying this formula to the first equation of the fractional-order system (6)–(9), we obtain the following equation:

$$\begin{aligned}
x_{j+1} - \sum_{i=1}^{j+1} e_i x_{j+1-i} - \mathfrak{r}_{j+1} x_0 &= \psi(\kappa)^\xi \rho^\xi - \psi(\kappa)^\xi \left(\beta_m^\xi \frac{z_{n-j}}{N} + \beta_\rho^\xi \frac{w_{n-j}}{N}\right) x_{j+1} e^{-\mu\tau} \\
&\quad - \psi(\kappa)^\xi \mu^\xi x_{j+1}.
\end{aligned} \tag{44}$$

Some calculations and simplifications lead to the following expression:

$$x_{j+1} = \frac{\sum_{i=1}^{j+1} e_i x_{j+1-i} + \mathfrak{r}_{j+1} x_0 + \psi(\kappa)^\xi \rho^\xi}{1 + \psi(\kappa)^\xi \left(\beta_m^\xi \frac{z_{n-j}}{N} + \beta_\rho^\xi \frac{w_{n-j}}{N}\right) e^{-\mu\tau} + \psi(\kappa)^\xi \mu^\xi} \tag{45}$$

In a similar fashion, we can obtain the following recursive formulas for the other three equations in the fractional-order system (6)–(9), for each $j \in \mathbb{N} \cup \{0\}$:

$$y_{j+1} = \frac{1}{1+\psi(\kappa)^{\xi}(\theta^{\xi}+\mu^{\xi})}\sum_{i=1}^{j+1} e_i y_{j+1-i} + \mathfrak{r}_{j+1}y_0 + \psi(\kappa)^{\xi}\left(\beta_m^{\xi}\frac{z_{n-j}}{N} + \beta_{\rho}^{\xi}\frac{w_{n-j}}{N}\right)y_j e^{-\mu\tau}, \tag{46}$$

$$z_{j+1} = \frac{1}{1+\psi(\kappa)^{\xi}\mu_m^{\xi}}\sum_{i=1}^{j+1} e_i z_{j+1-i} + \mathfrak{r}_{j+1}z_0 + \psi(\kappa)^{\xi} f^{\xi}\theta^{\xi} y_j, \tag{47}$$

$$w_{j+1} = \frac{1}{1+\psi(\kappa)^{\xi}\mu^{\xi}}\sum_{i=1}^{j+1} e_i w_{j+1-i} + \mathfrak{r}_{j+1}w_0 + \psi(\kappa)^{\xi}(1-f^{\xi})\theta^{\xi} y_j. \tag{48}$$

By using these last four algebraic equations and by employing mathematical induction, the proof for the following result is straightforward.

Theorem 7. *The discrete systems* (45)–(48) *preserve the positivity of the initial conditions.* □

Next, we prove the boundedness of the scheme.

Theorem 8. *The finite-difference scheme* (45)–(48) *preserves the boundedness of the solutions.*

Proof. By adding and rearranging (45)–(48), we obtain the following expression:

$$\begin{aligned}(x_{j+1}+y_{j+1}+z_{j+1}+w_{j+1}) &+ \psi(k)^{\xi}\left[\mu x_{j+1} + \left(\beta_m\frac{z_k}{N} + \beta_{\rho}\frac{w_k}{N}\right)x_{j+1}e^{-\mu\tau}\right.\\ &\left.+ (\theta+\mu)y_{j+1} + \mu_m z_{j+1} + \mu w_{j+1}\right] = \sum_{i=1}^{j+1} e_i(x_{j+1-i}+y_{j+1-i}+z_{j+1-i}+w_{j+1-i})\\ &+ r_{j+1}(x_0+y_0+z_0+w_0) + \psi(k)^{\xi}\left[\rho + \left(\beta_m\frac{z_k}{N} + \beta_{\rho}\frac{w_k}{N}\right)y_j e^{-\mu\tau}\right.\\ &\left.+ (f\theta + (1-f)\theta)y_j\right].\end{aligned} \tag{49}$$

The conclusion of this result is proved by using mathematical induction. Firstly, consider the case when $j = 0$ in (49) in order to obtain the following:

$$\begin{aligned}&\left[1+\psi(k)^{\xi}\left(\mu + \left(\beta_m\frac{z_k}{N} + \beta_{\rho}\frac{w_k}{N}\right)e^{-\mu\tau}\right)\right]x_1 + \left(1+\psi(k)^{\xi}(\theta+\mu)\right)y_1 + \left(1+\psi(k)^{\xi}\mu_m\right)z_1\\ &+ \left(1+\psi(k)^{\xi}\mu\right)w_1 = e_1\frac{\rho}{\mu} + r_1\frac{\rho}{\mu} + \psi(k)^{\xi}\left[\rho + \left(\beta_m\frac{z_k}{N} + \beta_{\rho}\frac{w_k}{N}\right)y_0 e^{-\mu\tau} + \theta y_0\right]\\ &= \left(\xi + \frac{1}{\Gamma(1-\xi)}\right)\frac{\rho}{\mu} + \psi(k)^{\xi}\left[\rho + \left(\beta_m\frac{z_k}{N} + \beta_{\rho}\frac{w_k}{N}\right)y_0 e^{-\mu\tau} + \theta y_0\right],\end{aligned} \tag{50}$$

If B_1 is the right-hand side of the equation above, then $x_1 < B_1$ when

$$1+\psi(k)^{\xi}\left(\mu + \left(\beta_m\frac{z_k}{N} + \beta_{\rho}\frac{w_k}{N}\right)e^{-\mu\tau}\right) > 1. \tag{51}$$

Similarly, it is easy to check that this constant is such that $y_1 < B_1$, $z_1 < B_1$ and $w_1 < B_1$. We define B_1 as the maximum of those constants. Now, if $j = 1$ in (49), we can readily check that

$$\begin{aligned} & x_2 + y_2 + z_2 + w_2 + \psi(k)^{\xi}\left[\mu x_2 + \left(\beta_m \frac{z_k}{N} + \beta_\rho \frac{w_k}{N}\right) x_2 e^{-\mu\tau} + (\theta + \mu) y_2 + \mu_m z_2 + \mu w_2\right) \\ & = e_1(x_1 + y_1 + z_1 + w_1) + e_2(x_0 + y_0 + z_0 + w_0) + r_2(x_0 + y_0 + z_0 + w_0) \\ & \quad + \psi(k)^{\xi}\left[\rho + \left(\beta_m \frac{z_k}{N} + \beta_\rho \frac{w_k}{N}\right) y_1 e^{-\mu\tau} + \theta y_1\right] \\ & < e_1\left(N_1 + \frac{\rho}{\mu}\right) + \frac{1}{\Gamma(1-\xi)} \frac{\rho}{\mu} + \psi(k)^{\xi}\left[\rho + \left(\beta_m \frac{z_k}{N} + \beta_\rho \frac{w_k}{N}\right) y_1 e^{-\mu\tau} + \theta y_1\right]. \end{aligned} \tag{52}$$

Here, $N_1 = 4B_1$. From the right-hand side, we can see that there is a constant B_2 with the property of $x_2 < B_2$, $y_2 < B_2$, $z_2 < B_2$ and $w_2 < B_2$. Proceeding inductively, we arrive at the conclusion. □

Before closing this section, we provide some numerical simulations to confirm the analytical and numerical results derived in this work. Three sets of simulations are provided. The first of two are simulations in which the disease-free and endemic scenarios are considered. In those cases, we use the parameter values summarized in Table 1.

Table 1. Parameters used for simulation purposes.

Parameters	Disease-Free Case	Endemic Case
ρ	0.5	0.5
β_ρ	1.3	2.3
β_m	1.5	2.5
θ	0.19	0.19
μ	0.5	0.5
f	0.7	0.7
τ	0.5	0.5

Example 1. *Let us consider the disease-free case as described by the parameters in Table 1. Computationally, we will approximate the solution to the continuous epidemic model using the numerical scheme introduced in the present manuscript. Moreover, as differentiation orders, we will consider* $\xi = 0.75, 0.8, 0.85,$ *and* 0.9. *Figure 1 provides the results of our simulations under these conditions. More precisely, the graphs depict the dynamics of (a) x vs. t, (b) y vs. t, (c) z vs. t, and (d) w vs. t. It is worth pointing out that the solutions all tend asymptotically to the disease-free equilibrium as time increases. This shows graphical proof that the derived disease-free of the analytical model is correct, and that the numerical model is capable of identifying this point correctly, as demonstrated by our results. Moreover, the finite-difference scheme is capable of identifying the stability of the equilibrium solution.*

Example 2. *We now consider the endemic scenario. To that end, we employ the parameter values in Table 1. The results of our simulations are presented in Figure 2, for various values of the differentiation order. Once more, we observe that the solutions for the four compartmental functions tend to the endemic equilibrium solution, independently of the differentiation order. This provides computational evidence that the scheme correctly identifies this constant solution of the analytical model. Moreover, we confirm the accurateness of our analytical derivations. In addition, the stability of this equilibrium is correctly identified qualitatively by the numerical model, as expected.*

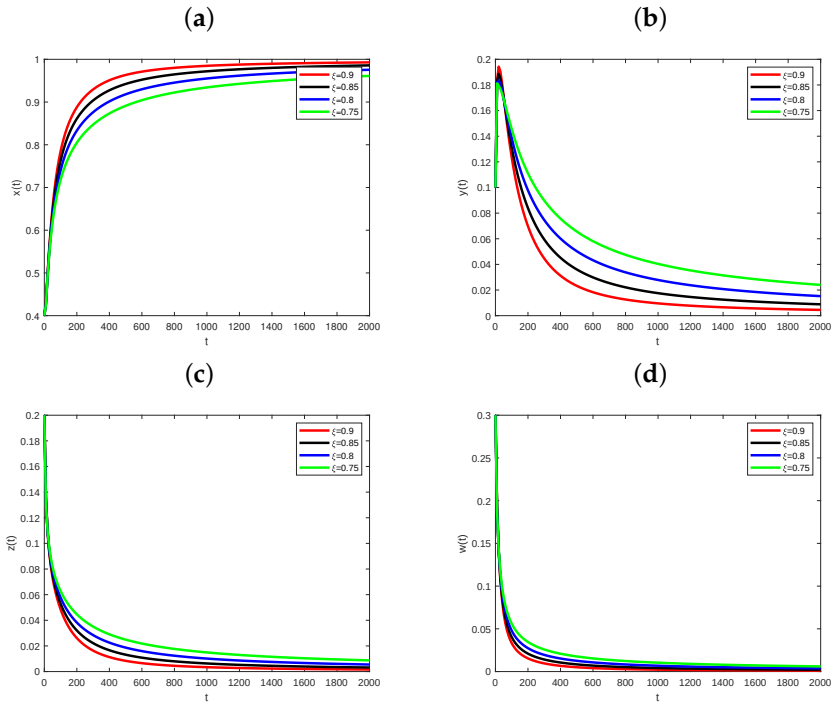

Figure 1. Graphs for the numerical solution of the fractional-order model investigated in this work. The graphs were obtained using the numerical method introduced in the previous section, and they provide the dynamics of (**a**) x vs. t, (**b**) y vs. t, (**c**) z vs. t, and (**d**) w vs. t. The parameters employed to produce these simulations were those provided in Table 1 for the disease-free case. As indicated by the legends, various differentiation orders ξ were employed.

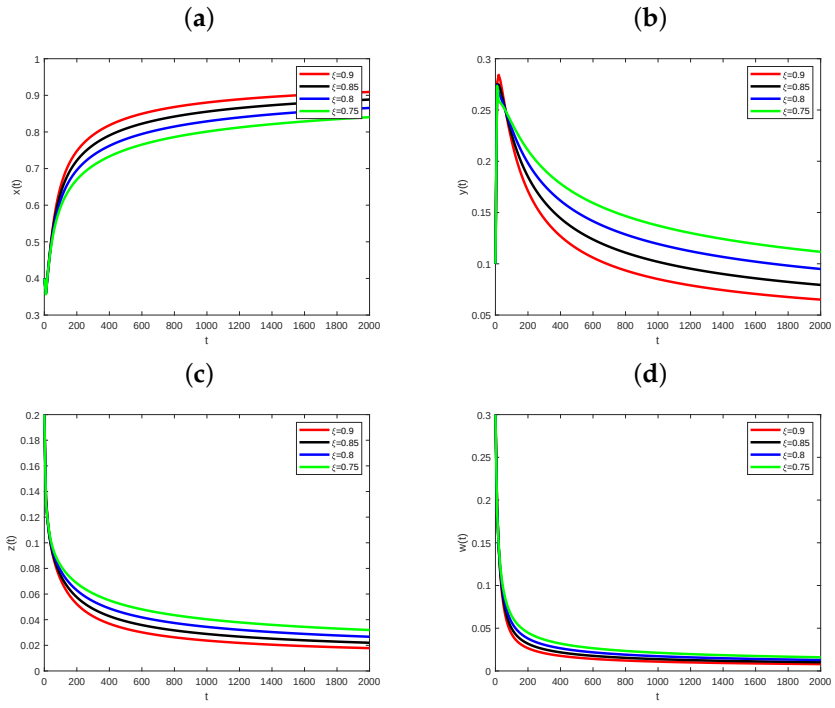

Figure 2. Graphs for the numerical solution of the fractional-order model investigated in this work. The graphs were obtained using the numerical method introduced in the previous section, and they provide the dynamics of (**a**) x vs. t, (**b**) y vs. t, (**c**) z vs. t, and (**d**) w vs. t. The parameters employed to produce these simulations were those provided in Table 1 for the endemic case. As indicated by the legends, various differentiation orders ξ were employed.

Example 3. *In our last example, we examine the effect of the delay parameters on the solution of the function y by assuming the endemic case. In this case, we employed the values of* 0.5, 0.8, 1.1, *and* 2 *for* τ, *and we observed the behavior of the solutions. The results are provided in Figure 3, and they show that the solution converges toward the equilibrium in all cases. The equilibria are dependent on* τ, *as established by the analytical results, and they are correctly identified by the numerical model. It is worth pointing out here that we used a differentiation order equal to* 0.9, *but that we also carried out more experiments. The results are not shown here to avoid redundancy, but they establish the validity of our analytical and numerical results.*

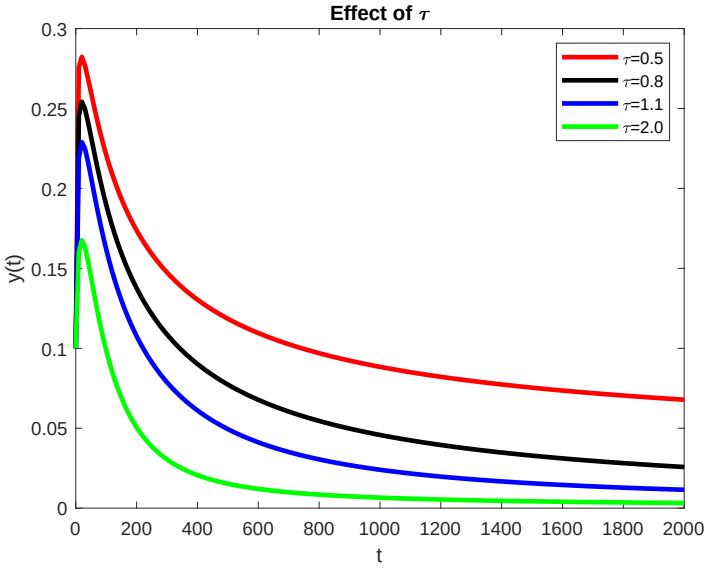

Figure 3. Graph of the effect of τ on $y(t)$ in the endemic case, as considered in Table 1. We used the delayed values provided in the legend of the graph and set a differentiation order equal to 0.9. To carry out the simulations, we used the numerical model presented in this work in order to approximate the solutions for the epidemic model under study.

5. Conclusions

A compartmental leprosy infection model was transformed into a fractional-order system for an alternative perception of the disease dynamics. The Caputo differential operator of order ξ was considered in order to investigate the different aspects of the infection propagation and solution variables. The positivity and the boundedness properties of the underlying model were analytically confirmed. Equilibrium points were derived and investigated in terms of their local and global stability. The basic reproductive number was calculated with the help of a new generation matrix technique. In turn, the Routh–Hurwitz criteria, a Lyapunov-type function, and the basic reproductive number were used to prove the local and global stability of the model at both steady states. To simulate the dynamics of this model, a numerical scheme was proposed to approximate the solutions. The proposed finite-difference scheme is positivity- and boundedness-preserving. It is worth noting that the scheme employed the Grünwald–Letnikov scheme to approximate the Caputo derivative, and it was designed using non-standard rules. The simulations presented in this work show that the numerical scheme assures the positivity and the boundedness of the solution. Moreover, we confirmed that the scheme converges towards the exact steady states of the fractional leprosy model, and that it correctly identifies their stability. In the last of our numerical results, we confirmed the fact that the delay factor could considerably control the propagation of the infection.

Author Contributions: Conceptualization, Z.I., N.A., and J.E.M.-D.; methodology, Z.I., N.A., and J.E.M.-D.; software, Z.I., N.A., and J.E.M.-D.; validation, Z.I., N.A., and J.E.M.-D.; formal analysis, Z.I., N.A., and J.E.M.-D.; investigation, Z.I., N.A., and J.E.M.-D.; resources, Z.I., N.A., and J.E.M.-D.; data curation, Z.I., N.A., and J.E.M.-D.; writing—original draft preparation, Z.I., N.A., and J.E.M.-

D.; writing—review and editing, Z.I., N.A., and J.E.M.-D.; visualization, Z.I., N.A., and J.E.M.-D.; supervision, J.E.M.-D.; project administration, J.E.M.-D.; funding acquisition, J.E.M.-D. All authors have read and agreed to the published version of the manuscript.

Funding: This research was funded by the National Council for Science and Technology of Mexico (CONATYT) through grant number A1-S-45928.

Institutional Review Board Statement: Not applicable.

Informed Consent Statement: Not applicable.

Data Availability Statement: The data are contained within the article.

Acknowledgments: The authors would like to thank Robert Kotiuga for his invaluable comments.

Conflicts of Interest: The authors declare no conflicts of interest.

References

1. Mazza, D.C.; Pastore, D.H.; De-Souza, F.D.M. Mathematical and computational and modeling for leprosy's dynamics. *Cereus* **2019**, *2*, 222–131. [CrossRef]
2. Peters, R.M.H.; Dadun, M.; Lusli, B.; Miranda-Galarza, W.H.; Brake, M.B.; Zweekhorst, M.; Damayanti, R.; Seda, F.; Bunders, J.F.; Irwanto, G. The meaning of leprosy and everyday experiences: An Exploration in Cirebon, Indonesia. *J. Trop. Med.* **2013**, *10*, 2013. [CrossRef] [PubMed]
3. De Matos, H.J.; Blok, D.J.; de Vlas, S.J.; Richardus, J.H. Leprosy new case detection trends and the future effect of preventive interventions in Pará State, Brazil: A Modelling Study. *PLoS Neglected Trop. Dis.* **2016**, *10*, e0004507. [CrossRef] [PubMed]
4. Chiyaka, E.T.; Muyendesi, T.; Nyamugure; Mutasa, F.K. Theoretical assessment of the transmission dynamics of Leprosy. *Sci. Res.* **2013**, *4*, 1–155. [CrossRef]
5. Mushayabasa, S.; Bhunu, C.P. Modelling the effects of chemotherapy and relapse on the transmission dynamics of leprosy. *Math. Sci.* **2012**, *6*, 1–12. [CrossRef]
6. Abubakar, U.Y.; Reju, S.A.; Awojoyogbe, B.O. Markov decision model and the application to the cost of treatment of leprosy disease. *Leonardo J. Sci.* **2007**, *11*, 69–78.
7. Enagi, A.I. A deterministic compartmental model of tuberculosis control strategy adopted by the national tuberculosis and leprosy control programme in Nigeria. *Pac. J. Sci. Technol.* **2013**, *14*, 342–348.
8. Lietman, T.; Porco, T.; Blower, S. Leprosy and tuberculosis: The epidemiological consequences of cross-immunity. *Am. J. Public Health* **2011**, *78*, 12. [CrossRef]
9. Walker, S.L.; Lockwood, D.N.J. The clinical and immunological features of leprosy. *Br. Med. Bullet.* **2006**, *77–78*, 103–121. [CrossRef]
10. Blok, D.J.; Sake, J.D.V.; Egil, A.J.; Richardus, H.J. Mathematical modelling of leprosy and its control. *Sci. Direct* **2015**, *87*, 33–51.
11. Smith, R.L. Proposing a compartmental model for leprosy and parameterizing using regional incidence in Brazil. *PLoS Neglected Trop. Dis.* **2016**, *10*, 1–14. [CrossRef] [PubMed]
12. Hohmann, N.; Voss-Böhme, A. The epidemiological consequences of leprosy-tuberculosis co-infection. *Math. Biosci.* **2013**, *241*, 225–237. [CrossRef] [PubMed]
13. Meima, A.; Gupte, M.D.; Van Oortmarssen, G.J.; Habbema, J.D.F. SIMLEP: A simulation model for leprosy transmission and control. *Int. J. Lepr. Other Mycobact. Dis.* **1999**, *67*, 215–236. [PubMed]
14. Donoghue, H.D.; Marcsik, A.; Molnar, E.; Palfi, G. A migration-driven model for the historical spread of leprosy in medieval Eastern and Central Europe. *Infect. Genet. Evol.* **2015**, *31*, 250–256. [CrossRef] [PubMed]
15. Haroun, O.M.O.; Vollert, J.L.D.N.; Bennett, D.L.H.; Pai, V. Clinical characteristics of neuropathic pain in leprosy and associated somatosensory profiles. *Deep. Phenotyping Study India Pain Rep.* **2019**, *4*, 743.
16. Barros, L.C.D.; Lopes, M.M.; Pedro, F.S.; Esmi, E.; Santos, J.P.C.D.; Sánchez, D.E. A fractional-order model of HIV infection: Numerical solution and comparisons with data of patients. *Int. J. Biomath.* **2021**, *40*, 1–21.
17. Arafa, A.A.M.; Rida, S.Z.; Khalil, M. The memory effect on fractional calculus: An application in the spread of COVID-19. *Comput. Appl. Math.* **2014**, *7*, 1450036.
18. Huang, C.; Wang, J.; Chen, X.; Cao, J. Bifurcations in a fractional-order BAM neural network with four different delays. *Neural Networks* **2021**, *141*, 344–354. [CrossRef]
19. Huang, C.; Liu, H.; Shi, X.; Chen, X.; Xiao, M.; Wang, Z.; Cao, J. Bifurcations in a fractional-order neural network with multiple leakage delays. *Neural Netw.* **2020**, *131*, 115–126. [CrossRef]
20. Li, P.; Li, Y.; Gao, R.; Xu, C.; Shang, Y. New exploration on bifurcation in fractional-order genetic regulatory networks incorporating both type delays. *Eur. Phys. J. Plus* **2022**, *137*, 598. [CrossRef]
21. Tulu, T.W.; Tian, B.; Wu, Z. Modeling the effect of quarantine and vaccination on Ebola disease. *Adv. Differ. Equations* **2017**, *2017*, 178. [CrossRef]
22. Lakshmikantham, V.; Leela, S.; Martynyuk, A.A. *Stability Analysis of Non-Linear System*, 2nd ed.; Springer: New York, NY, USA, 1989.

23. Huo, H.F.; Feng, L.X. Global stability for an HIV/AIDS epidemic model with different latent stages and treatment. *Appl. Math. Model.* **2013**, *37*, 1480–1489. [CrossRef]
24. Scherer, R.; Kalla, S.; Tang, Y.; Huang, J. The Grunwald-Letnikov method for fractional differential equations. *Comput. Math. Appl.* **2011**, *62*, 902–907. [CrossRef]
25. Mickens, R.E. Dynamic consistency: A fundamental principle for constructing nonstandard finite difference schemes for differential equations. *J. Differ. Equ. Appl.* **2005**, *11*, 645–653. [CrossRef]

Disclaimer/Publisher's Note: The statements, opinions and data contained in all publications are solely those of the individual author(s) and contributor(s) and not of MDPI and/or the editor(s). MDPI and/or the editor(s) disclaim responsibility for any injury to people or property resulting from any ideas, methods, instructions or products referred to in the content.